International Forum on Aeroelasticity and Structural Dynamics
IFASD 2024
17-21 June 2024, The Hague, The Netherlands

# ON THE PREPARATION OF A FLEXIBLE REAL-TIME AIRCRAFT MODEL FOR A FLIGHT SIMULATOR

**Gefferson C. Silva[1], Bernd Boche[1], Hannes Wilke[1], Flavio J. Silvestre[1]**

[1]Technical University of Berlin
Marchstraße 12, 10587 Berlin, Germany
g.silva@tu-berlin.de
flavio.silvestre@tu-berlin.de

**Keywords:** real-time simulations, flexible aircraft, computational costs, flight simulator

**Abstract:** Before flight test campaigns are pursued, handling qualities analyses of new aircraft designs are typically performed by means of a pilot-in-the-loop full-flight simulator. This also includes the forthcoming generation of greener aircraft, for which environmental damages resulting from aircraft emissions is mitigated. However, this type of air-vehicle requires special treatment in flight dynamics modeling and simulation, due to the interactive coupling between rigid-body dynamics and aeroelasticity. The extended model simulations result in an expressive increase in computational costs, which makes real-time simulations of flexible aircraft a current challenge. Therefore, the work at hand discusses an approach to reduce the computational consumption required for simulating slightly flexible aircraft models, in order to be embedded into a flight simulator. The mean-axes formulation is used to represent the coupled relations between flight mechanics and flexibility effects. The incremental forces and moments expressions are then modified algebraic-wise to obtain an equivalent but computationally efficient formulation to those expressions.

## 1 INTRODUCTION

Aiming at mitigating flight-related emissions, modern aircraft are set to present higher efficiency by minimizing the lift-to-drag ratio needed for long-haul flights. In short, future aircraft are intended to combine an enhanced performance with an accentuated reduction in fuel consumption, hence reducing carbon dioxide footprint. In the face of these economic and ecological constraints, two major strategies have been investigated in recent decades within the aeronautical community: the use of lighter materials, usually constituted of carbon-fiber laminates and the design of elongated or high-aspect-ratio wings. The extensive use of composites reduces the aircraft's overall weight, while elongated wings result in a considerable cut in the induced drag. However, these methodologies lead to aircraft with increased flexibility, the so-called flexible aircraft.

As the main drawbacks, flexible aircraft models can no longer stand the assumption of rigid-body and the inclusion of elastic effects is required. Consequently, flight simulations involving this type of aircraft typically demand higher computational costs compared to simulating a rigid aircraft. The latter is a result of the fact that the extension of classical models to incorporate the mutual interaction between aeroelasticity and rigid-body dynamics inflates the number of equations to be solved. In addition, aeroelastic controllers may also introduce additional numerical costs and complexity to the system, as per in [1, 2]. Notch filters, commonly used in

closed-loop to suppress the undesirable elastic dynamics, may become inadequate. With the small separation between rigid-body and elastic frequencies, the use of notch filters can yield low-performance controllers [3].

Furthermore, Pilot Induced Oscillations (or just PIO) may also occur as a result of structural flexibility effects, thereby affecting the overall vehicle maneuverability, as in [4, 5]. When structural vibrations present a bandwidth close enough to the pilot's biodynamics, involuntary inputs may be produced or commanded through [6, 7]. Aeroelastic stability and gust rejection aspects are also of great concern for flexible aircraft designers. Such responses are key points in the evaluation process of the vehicle, bringing additional carefulness during the aircraft's model validation [8]. Together, all these downsides have a direct impact on pilot-in-the-loop simulators and on handling quality assessments [9], substantiating deeper involvement in flexible aircraft research topics.

The formulations currently available for modeling the behavior of flexible aircraft present a great range of complexity and hence computational costs, depending on the aircraft's level of flexibility, as reported in [10–12]. In order to reduce this price, model-order reduction techniques have been employed to minimize the number of states of such models and the consequent computational costs [13,14]. However, in principle, real-time simulations of flexible aircraft are still a nowadays obstacle, and there is plenty of room for further investigations. These tools can be embedded into flight simulators, bringing advantages that go beyond design reasons. Applications for that range from control and model validations up to adequate piloting training, as they permit pilots to fly with maximum safety while reducing costs, e.g. related to flying prototypes [15].

An ongoing example in this regard is the research project WISDOM (Wing Integrated Systems Demonstration On Mechatronic rig), where the Technical University Berlin (TUB) along with the German Aerospace Center (DLR), Liebherr and FFT are interested in investigating how elastic effects may affect the aircraft handling qualities. For that, two full-flight simulators are planned to be used: the flight simulator SEPHIR, from the TUB, and the DLR full-motion simulator AVES. Different controllers with diverse objectives are also intended to be analyzed within pilot-in-the-loop tests, expecting to deliver important insights about the controllability, stability, and handling qualities of the WISDOM reference aircraft. To be able to evaluate these effects during the flight tests at SEPHIR and AVES, it is mandatory to simulate the interaction between the rigid-body dynamics and the aeroelastic flexibility in real time.

Motivated by this scenario, this paper discusses the preparation and evaluation of a flexible aircraft model to be embedded into the flight simulator SEPHIR within the project WISDOM. The model representation is based on the linearized mean-axes formulation, coupled to an unsteady strip theory method in the time domain, as per in [12]. A series of modifications in the set of equations is proposed to minimize the number of computational operations required and hence reach real-time capabilities based on the work developed by Paulino [15]. In short, no model-order reduction method is applied, and instead, these modifications are done so that computational costly terms become time-invariant, which means they can be evaluated before the simulation (offline), saving computational effort. Finally, simulation time histories comparing time responses and computational costs are analyzed.

## 2 AIRCRAFT MODEL

The WISDOM reference aircraft is expected to visualize and demonstrate the implementation of the aeroelastic functions and their effects on the entire aircraft in the flight simulator. The configuration was projected to meet current and realistic business cases for a commercial aircraft. Therefore, the aircraft, the so-called D2AE configuration, is a short and medium-haul configuration for around 240 passengers. The model design was done by the DLR in order to be able to address scientific questions about aeroelasticity and to undertake further considerations on the topics of flight mechanics, load analysis, structural design, and multidisciplinary optimization [16].

This configuration presents significant development in the wing design, with its higher aspect ratio and span. In addition, a pair of split ailerons consisting of a total of 6 independent aileron surfaces was applied. Adding to it, the wing is still equipped with two pairs of flaps, which allows the allocation of different control strategies to the diverse control surfaces available, as depicted in Fig. 1. The structural model is such that a flutter in the range of 6-7 Hz is achieved, and a set of 50 elastic modes of low to medium frequencies are available to be used within the aeroelastic model. These frequencies vary from about 2 to 25 Hz; as a consequence, a flight mechanical model that takes into account the coupled aeroelastic effects is needed.

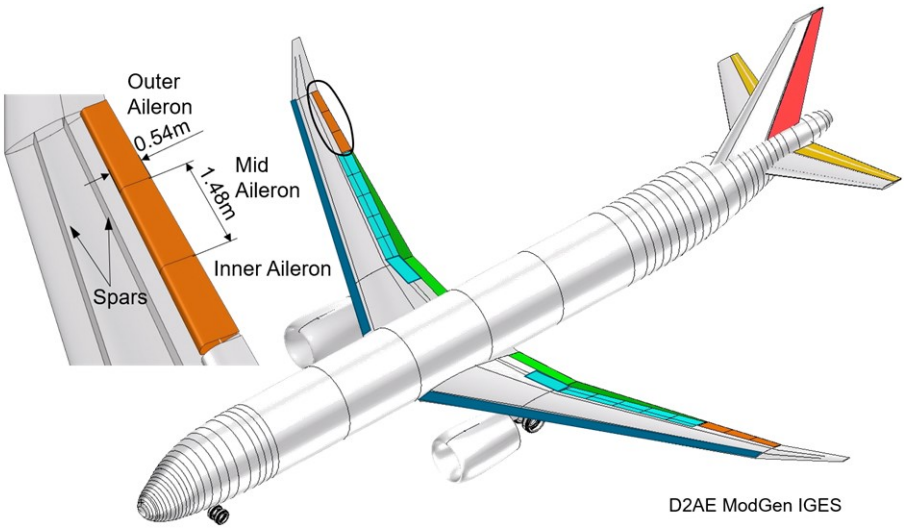


Figure 1: D2AE configuration. [16]

For that, the aircraft dynamics are written based on the linearized mean axes constraints, i.e., the inertial couplings between rigid-body and elastic degrees of freedom are disregarded. The structural dynamics are linearly represented in terms of the in-vacuum orthogonal elastic modes of the vehicle. Here, the elastic database results from an FE model modal analysis, once no ground vibration tests are conducted in WISDOM. With that, the principle of superposition is applied, thus resulting in a set of linear second-order differential equations in the modal coordinates.

To determine the incremental aerodynamics, due to elastic deformations, an unsteady Strip Theory formulation in the time domain is used. The induced forces and moments are calculated by employing the exponential approximation for the Wagner function [17], proposed by Jones [18]. In addition, Yates' modified strip analysis method [19] is used to modify the lift curve slope and aerodynamic center position for each strip so that finite span aerodynamic effects are taken into account. The final system of equations is composed of the rigid-body equations of

motion, including the incremental aerodynamics induced by the aircraft flexibility, added by the structural dynamics equations and a set of aerodynamic lag dynamic equations [12].

The equations of unsteady motion experienced by a rigid aircraft, here represented by a six-degrees-of-freedom model written in the body coordinate system along with the kinematic and position equations, can be expressed as

$$\dot{\mathbf{V}}_B = -\boldsymbol{\omega}_B \times \mathbf{V}_B + \mathbf{T}_{BI}\mathbf{G}_I + \frac{1}{m}\mathbf{F^{ext}}_B \,, \tag{1}$$

$$\dot{\boldsymbol{\omega}}_B = -\mathbf{J}^{-1}(\boldsymbol{\omega}_B \times (\mathbf{J}\boldsymbol{\omega}_B)) + \mathbf{J}^{-1}\mathbf{M^{ext}}_B \,, \tag{2}$$

$$\dot{\boldsymbol{\theta}} = \mathbf{S}^{-1}(\boldsymbol{\theta})\boldsymbol{\omega}_B \,, \tag{3}$$

$$\dot{\mathbf{r}}_I = \mathbf{T}_{BI}^T \mathbf{V}_B \,. \tag{4}$$

Equations 1 and 2 describe the respective translational and rotational dynamics of the aircraft, i.e., $\mathbf{V}_B = [u,\ v,\ w]$ and $\boldsymbol{\omega}_B = [p,\ q,\ r]$. In addition, $\mathbf{T}_{BI}$ is the transformation matrix from the inertial frame to the body reference frame, $\mathbf{G}_I$ is the aircraft weight vector, and $m$ and $\mathbf{J}$ are the aircraft total mass and inertia matrix, respectively. $\mathbf{F^{ext}}_B$ and $\mathbf{M^{ext}}_B$ represents the total external forces and moments acting on the aircraft, which in this case includes propulsion loads, rigid-body-related loads, and incremental aerodynamic loads due to elastic effects, such as

$$\mathbf{F^{ext}}_B = (\mathbf{F^{ae}}_{rb} + \mathbf{F^{ae}}_{flex} + \mathbf{F^{prop}})_B \,, \tag{5}$$

$$\mathbf{M^{ext}}_B = (\mathbf{M^{ae}}_{rb} + \mathbf{M^{ae}}_{flex} + \mathbf{M^{prop}})_B \,, \tag{6}$$

where $[\ ]^{\mathbf{ae}}{}_{rb}$ are the rigid-body-related loads, $[\ ]^{\mathbf{ae}}{}_{flex}$ represent the incremental aerodynamic loads, and at last $[\ ]^{\mathbf{prop}}$ are the propulsion loads.

To complement, Eqs. 3 and 4 represent the respective kinematic relations and position dynamics of the aircraft. Therefore, in these expressions, $\boldsymbol{\theta} = [\phi,\ \theta,\ \psi]$ and $\mathbf{r}_I = [x_E,\ y_E,\ z_E]$, and $\mathbf{S}$ is the matrix relating Euler angles rates and the body angular rates.

The extension of the aircraft rigid-body model, to include elastic effects, permits one to simulate the complete aircraft behavior, including local deformations of the main lifting surfaces wing and empennages. To this matter, a modal superposition technique is ergo assumed, resulting in a set of structural dynamic equations. Here, the generalized forces $\mathbf{Q}_\eta$ acting on the airframe are also resulting from unsteady aerodynamic loads in the time-domain. Additionally, the aerodynamic lag states are modeled via the Jones approximation for the Wagner function. These assumptions together define the following set of aeroelastic dynamic equations:

$$\ddot{\boldsymbol{\eta}} = -2\boldsymbol{\xi}\boldsymbol{\omega_n}\dot{\boldsymbol{\eta}} - \boldsymbol{\omega_n}^2\boldsymbol{\eta} + \boldsymbol{\mu}^{-1}\mathbf{Q}_\eta \,, \tag{7}$$

$$\dot{\boldsymbol{\lambda}} = \boldsymbol{\Lambda}\boldsymbol{\lambda} + \boldsymbol{\Upsilon}\dot{\mathbf{w}}_{3/4} \,, \tag{8}$$

in which $\boldsymbol{\eta}$ is the vector of modal coordinates, $\boldsymbol{\lambda}$ is the vector containing the aerodynamic lags, and $\dot{\mathbf{w}}_{3/4}$ represents the downwash acceleration at the three-quarter chord position. Moreover, $\boldsymbol{\Lambda}$ and $\boldsymbol{\Upsilon}$ are time-variant and static matrices that carry the properties of Jones's approximation equations.

The incremental forces and moments due to elastic deformations, as given in Eqs. 5 and 6, can also be written as a function of the modal coordinates and its derivatives, as well as the aerodynamic lags. The expression for the total incremental aeroelastic loads can then be written as:

$$\mathbf{F^{ae}}_{flex} = \rho\mathbf{F}^{(nc)}_{A\ddot{\eta}}\ddot{\boldsymbol{\eta}} + \rho V\left(\mathbf{F}^{(nc)}_{A\dot{\eta}} + \mathbf{F}^{(c)}_{A\dot{\eta}}\right)\dot{\boldsymbol{\eta}} + \rho V^2\mathbf{F}^{(c)}_{A\eta}\boldsymbol{\eta} + \rho V\mathbf{F}^{(c)}_{A\lambda}\boldsymbol{\lambda}\,, \tag{9}$$

$$\mathbf{M^{ae}}_{flex} = \rho\mathbf{M}^{(nc)}_{A\ddot{\eta}}\ddot{\boldsymbol{\eta}} + \rho V\left(\mathbf{M}^{(nc)}_{A\dot{\eta}} + \mathbf{M}^{(c)}_{A\dot{\eta}}\right)\dot{\boldsymbol{\eta}} + \rho V^2\left(\mathbf{M}^{(nc)}_{A\eta} + \mathbf{M}^{(c)}_{A\eta}\right)\boldsymbol{\eta} + \rho V\mathbf{M}^{(c)}_{A\lambda}\boldsymbol{\lambda}\,, \tag{10}$$

where $\rho$ is the air density and $V$ is the aircraft velocity. In addition, the circulatory and non-circulatory matrices, represented by the respective superscripts $(c)$ and $(nc)$ (as proposed in [17]), can be obtained by discretizing the lifting surfaces in a finite number of strips. Then, every individual contribution is summed to yield the overall aircraft incremental forces.

A complete description of the aeroelastic and incremental aerodynamic formulation applied here can be found in Ref. [12]. The latter contains the expressions for all the terms composing Eqs. 7 to 10. However, the classical formulation presented in the mentioned work is expensive computational-wise because of the number of computations required by the aeroelastic and incremental loads model in each time step. For example, the terms involved in the expressions above, for incremental loads, are calculated to have dimensions in the order of the number of strips $\times$ number of aeroelastic loads. All these terms, plus all the terms connected to the aeroelastic model, including the computation of the generalized forces, result in a time-consuming aeroelastic/extended approach.

Paulino [15] has shown that although highly nonlinear, rigid-body equations of motion are fast enough for real-time simulation. On the other hand, the incremental unsteady aeroelastic equations are very computationally expensive, being responsible for about 96% of the total simulation time. Meanwhile, computations rigid-body-related are responsible for about only 4% of the total simulation time. According to the mentioned author, this scenario suggests computationally efficient forms to calculate the incremental aeroelastic as worthwhile, whereas rigid-body computations may be kept unmodified to preserve computationally inexpensive nonlinearities, thus increasing model accuracy.

Based on that, and exploring the algebraic modifications proposed in [15], time-invariant computations can be detached from the time-dependent variables. This procedure can be applied to the different terms constituting the incremental forces and moments and the generalized forces. However, in this separation, the terms must be calculated per lifting surface, because strip-wise invariant transformations (in a particular surface) are therefore detached from the summations over the number of strips. To exemplify the mentioned approach, consider now the original expression for the circulatory moment coefficient related to $\dot{\boldsymbol{\eta}}$ and applied to a single $i$-th, as given in Ref. [12]:

$$\mathbf{M}^{(c)}_{A\dot{\eta}i} = \sum_{j=1}^{n_{si}}\left\{\mathbf{T}_{B^{(G)}B^{(L)}}\begin{bmatrix}0\\1\\0\end{bmatrix}\boldsymbol{m}^{(c)}_{\dot{\boldsymbol{\eta}}}(y_j) + \hat{\boldsymbol{\aleph}}_j\mathbf{T}_{B^{(G)}B^{(L)}}\mathbf{T}_{B^{(L)}A^{(L)}}(t)\begin{bmatrix}0\\0\\-1\end{bmatrix}\boldsymbol{l}^{(c)}_{\dot{\boldsymbol{\eta}}}(y_j)\right\}\Delta y_j, \tag{11}$$

where $\boldsymbol{\aleph}_j$ represents the non-deformed position of the elastic axis in the $j$-th strip regarding the aircraft center of mass, while $\hat{\boldsymbol{\aleph}}_j$ denotes the skew-symmetric matrix of $\boldsymbol{\aleph}_j$. Moreover,

$\mathbf{T}_{B^{(G)}B^{(L)}}$ represents the transformation matrix from local to global body reference frame, and $\mathbf{T}_{B^{(L)}A^{(L)}}$ is the time-dependent transformation matrix from the local aerodynamic to the local body reference frame. To complete, $\boldsymbol{l}^{(c)}_{\dot{\boldsymbol{\eta}}}(y_j)$ and $\boldsymbol{m}^{(c)}_{\dot{\boldsymbol{\eta}}}(y_j)$ are the strip circulatory coefficients for lift and pitching moment, respectively, related to $\dot{\boldsymbol{\eta}}$.

In the prior expression, the first part of the summation is already time independent and can therefore be calculated a priori. Nevertheless, the second part presents additional complications, since the time-variant term $\mathbf{T}_{B^{(L)}A^{(L)}}$ is placed in the middle of the expression. This results in a locked expression where the strip-dependent term cannot be detached from the summation to be also calculated beforehand. Thus, aiming at performing an algebraic simplification that results in a more efficient computation, the matrix product can be transformed as a vector cross-product. Moreover, using the cross-product anticommutative property [15], it results in:

$$\hat{\boldsymbol{\aleph}}_j \mathbf{T}_{B^{(G)}B^{(L)}} \mathbf{T}_{B^{(L)}A^{(L)}} \begin{bmatrix} 0 \\ 0 \\ -1 \end{bmatrix} = -\left( \mathbf{T}_{B^{(G)}B^{(L)}} \mathbf{T}_{B^{(L)}A^{(L)}} \begin{bmatrix} 0 \\ 0 \\ -1 \end{bmatrix} \right) \times \boldsymbol{\aleph}_j \,. \tag{12}$$

After performing such algebraic manipulation, Eq. 11 can be rewritten as:

$$\begin{aligned} \mathbf{M}^{(c)}_{A\dot{\eta}i} \;=\; & \sum_{j=1}^{n_{si}} \left\{ \mathbf{T}_{B^{(G)}B^{(L)}} \begin{bmatrix} 0 \\ 1 \\ 0 \end{bmatrix} \boldsymbol{m}^{(c)}_{\dot{\boldsymbol{\eta}}}(y_j) \right\} \Delta y_j \\ & -\text{skew}\left( \mathbf{T}_{B^{(G)}B^{(L)}} \mathbf{T}_{B^{(L)}A^{(L)}}(t) \begin{bmatrix} 0 \\ 0 \\ -1 \end{bmatrix} \right) \sum_{j=1}^{n_{si}} \left\{ \hat{\boldsymbol{\aleph}}_j \boldsymbol{l}^{(c)}_{\dot{\boldsymbol{\eta}}}(y_j) \right\} \Delta y_j \,, \end{aligned} \tag{13}$$

or in a more compact form as:

$$\mathbf{M}^{(c)}_{A\dot{\eta}i} = \mathbf{M}^{(c)(1)}_{A\dot{\eta}i} - \text{skew}\left( \mathbf{T}_{B^{(G)}B^{(L)}} \mathbf{T}_{B^{(L)}A^{(L)}}(t) \begin{bmatrix} 0 \\ 0 \\ -1 \end{bmatrix} \right) \mathbf{M}^{(c)(2)}_{A\dot{\eta}i} \,. \tag{14}$$

A similar procedure can be applied to the time-dependent "locked" terms in the different incremental forces and moments expressions; and also, to the generalized forces' expressions. With that, the summations over the number of strips, which represent a great part of the computational consumption, become time-invariant and can be calculated before the simulation, as an initial offline step. Consequently, the processing effort during the simulation is largely reduced. This approach can be mathematically represented as follows:

$$\begin{aligned} \mathbf{F}^{\mathbf{ae}}{}_{flex} &= \mathbf{F}^{\mathbf{ae}(nc)}(t) + \mathbf{F}^{\mathbf{ae}(c)}(t) \;\longrightarrow\; \mathbf{c}\bar{\mathbf{F}}^{\mathbf{ae}(nc)}\bar{\mathbf{F}}^{\mathbf{ae}(nc)}(t) + \mathbf{c}\bar{\mathbf{F}}^{\mathbf{ae}(c)}\bar{\mathbf{F}}^{\mathbf{ae}(c)}(t) \\ \mathbf{M}^{\mathbf{ae}}{}_{flex} &= \mathbf{M}^{\mathbf{ae}(nc)}(t) + \mathbf{M}^{\mathbf{ae}(c)}(t) \longrightarrow\; \mathbf{c}\bar{\mathbf{M}}^{\mathbf{ae}(nc)}\bar{\mathbf{M}}^{\mathbf{ae}(nc)}(t) + \mathbf{c}\bar{\mathbf{M}}^{\mathbf{ae}(c)}\bar{\mathbf{M}}^{\mathbf{ae}(c)}(t) \\ \mathbf{Q}_\eta &= \mathbf{Q}^{(nc)}_\eta(t) + \mathbf{Q}^{(c)}_\eta(t) \;\longrightarrow\; \mathbf{c}\bar{\mathbf{Q}}^{(nc)}_\eta\bar{\mathbf{Q}}^{(nc)}_\eta(t) + \mathbf{c}\bar{\mathbf{Q}}^{(nc)}_\eta\bar{\mathbf{Q}}^{(nc)}_\eta(t) \end{aligned} \tag{15}$$

where $\mathbf{c}\bar{\square}$ denote the pre-calculated aeroelastic and incremental aerodynamic terms. These offline calculations represent great majority of calculations resulting from the extension of a classical model to encompass the aircraft flexibility effects. A detailed description of this strategy is offered in [15].

## 3 RESULTS

The modeling formulation described above is applied to the reference aircraft developed within the WISDOM project. Therefore, the simulation architecture developed here in Matlab/Simulink to numerically obtain the overall dynamic characteristics of this virtual aircraft, in a non-real-time fashion, is given in more detail in Fig. 2. The latter shows the mutual interaction between the aircraft rigid-body dynamics, employing the six-degree-of-freedom equations of motion, and the aeroelastic and aerodynamic lag dynamics, generically illustrated as a block diagram.

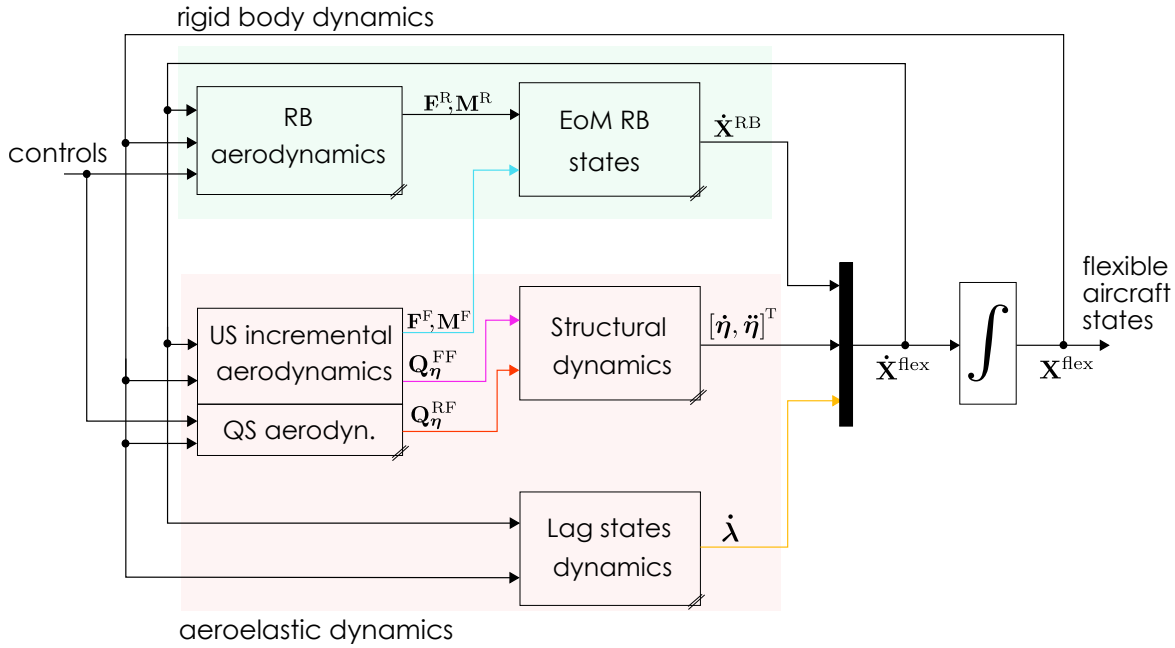


Figure 2: Schematical block diagram of the simulation environment

In short, based on the aircraft state and the elastic dynamics, the span-wise downwash can be determined, as well as the acceleration associated therewith. The strip-wise aerodynamic lag acceleration can then be calculated and inputted into the unsteady incremental aerodynamic calculation. Moreover, the rigid-body dynamics provides the aeroelastic dynamics with the aircraft state and control variables, and the aeroelastic dynamics provides the flight mechanics with the incremental aerodynamic forces and moments because of the elastic deformations.

With this simulation tool, the resulting flight dynamics of the flexible reference aircraft can then be trimmed and linearized under different flight conditions. Based on the linearized state matrix, the stability of the system can then be determined. Simple linear and non-linear simulations can be performed, and stability analysis can be evaluated under different options: considering the aircraft as a rigid-body, i.e., the classical flight mechanics applies; using quasi-steady incremental aerodynamics due to elastic deflections and rotations; using the full classical unsteady method given in [12]; or by using the modified approach described above.

By implementing the formulation presented in this section, a significant reduction in simulation time was obtained. In addition, once the proposed algebraic modifications result in an exact representation of the original formulation, the same response was also obtained, as shown in Fig. 3. The latter shows the nonlinear aircraft response undergoing a straight leveled trimmed flight at Mach 0.9 and an altitude of 8000 meters. A 3-degree doublet is then applied to the elevator.

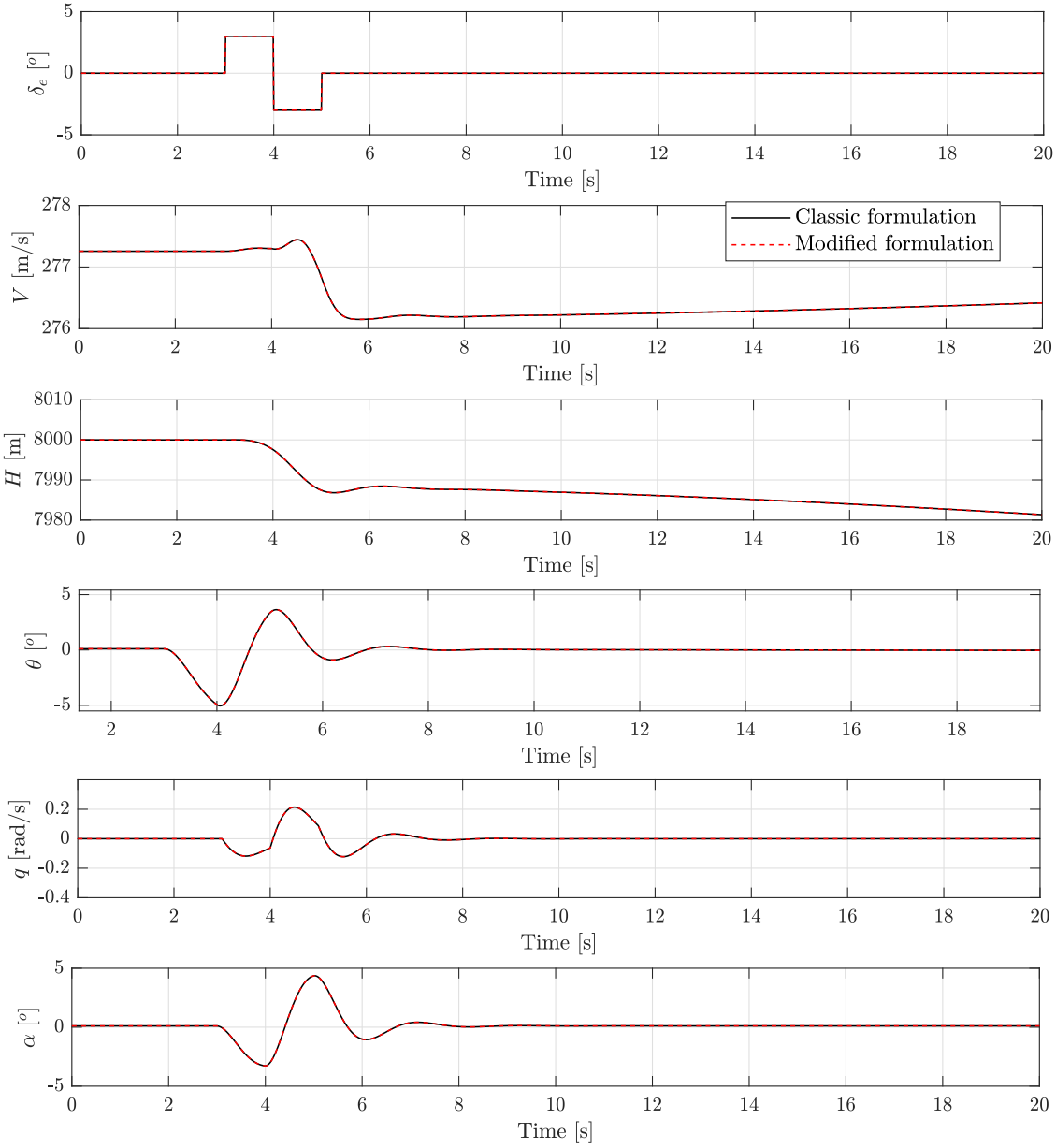


Figure 3: Nonlinear response to a 3-degree elevator doublet.

For this case, Fig. 4 depicts the 2D deformations of the aircraft airframe by using both classical and modified methodologies, which shows that the aeroelastic responses for the distinct formulations are also correspondent. In addition, the average simulation time measured for the WISDOM aircraft model, flying on a 20-second cruise, was 18.07 seconds. This represents a ratio of 0.903 seconds per simulated second, i.e., faster than real-time. In the same case, the original formulation resulted in a total simulation time of 123.98 seconds, which denotes a relation of 6.19 s/s. This represents a reduction of about 7 times in total time consumption.

However, this value was obtained by assuming 10 assumed modes, from a pool of 50 available modes. Therefore, to investigate how the number of assumed modes affects the total simulation time and hence the real-time capabilities of the algorithm, diverse simulations with different numbers of modes were performed. Table 1 shows the relation between the real-time aptitude of the model and the number of modes or states used. Real-time is then reached for up to about 20 assumed modes. Using the full modal basis, with 50 modes, the pre-calculated model

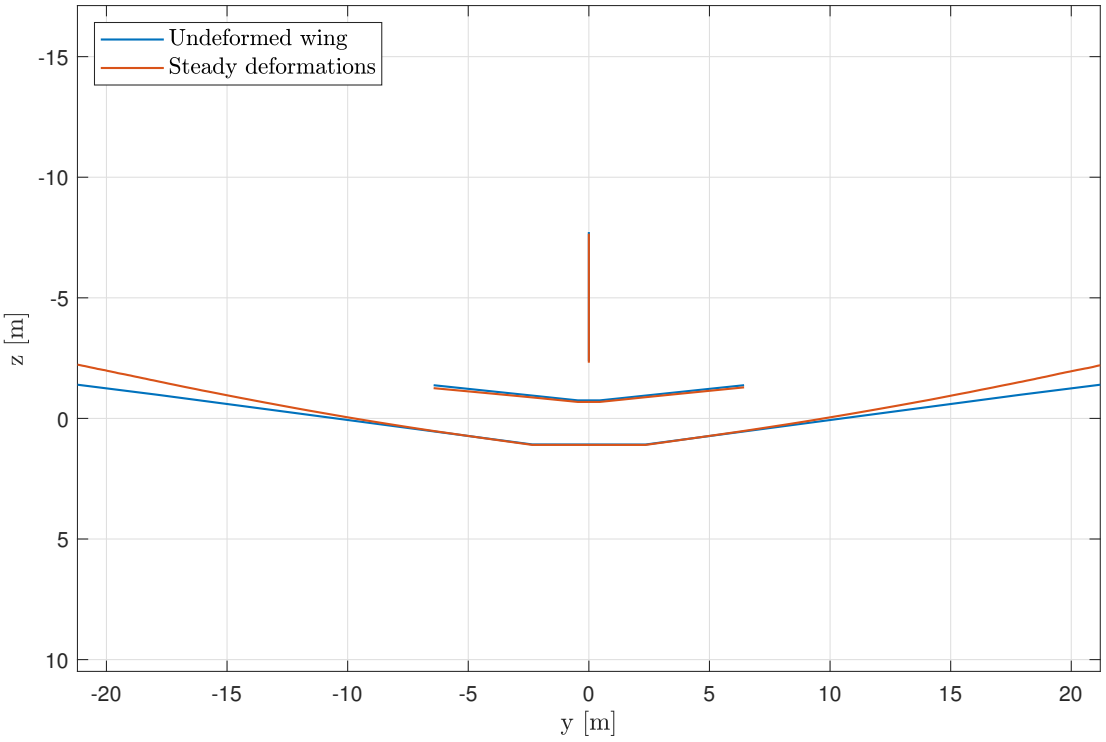


Figure 4: Airframe 2D steady deformations.

presents a relation of around 1.6 seconds per simulated second, which is still largely smaller than the full model one, which takes about 18.5 times more time. However, for this analysis, the number of aeroelastic strips, which also contribute to the final number of states, was not varied.

Table 1: The relation between computational costs and the number of assumed modes.

| | **nm = 10** | | **nm = 20** | | **nm = 30** | | **nm = 50** | |
|---|---|---|---|---|---|---|---|---|
| | **Orig.** | **Mod.** | **Orig.** | **Mod.** | **Orig.** | **Mod.** | **Orig.** | **Mod.** |
| **total time [s]** | 64.21 | 9.23 | 105.91 | 10.12 | 228.96 | 14.84 | 348.19 | 18.76 |
| **time/sim. time [-]** | 6.42 | 0.92 | 10.59 | 1.01 | 22.89 | 1.48 | 34.81 | 1.87 |
| **reduction factor** | 6.98 | | 10.09 | | 15.46 | | 18.60 | |

## 4 CONCLUSIONS

In future low-emission aircraft configurations, wings with a higher aspect ratio are expected. This leads to a reduction in the stiffness of the wing, potentiating the aircraft's flexibility. This fact can lead to high local loads when flying through turbulent atmospheres and, in extreme cases, to flutter and the associated loss of structural integrity. Since the practical implementation of active flutter suppression systems for civil aircraft involves the breaking of new technological ground, the joint project WISDOM aims to optimize and demonstrate the implementation of new flight control systems and control functions. For that a flight mechanical model that accounts for the coupled relation between flight dynamics and aeroelastic dynamics is necessary. However, the extended model results in an expressive increase in the total computational cost, which makes real-time simulations of flexible aircraft a current challenge. Therefore, the work at hand discussed an approach to reduce the computational consumption required for simulating slightly flexible aircraft models. The incremental forces and moments expressions were

modified to obtain an equivalent but computationally more efficient formulation.

The results showed a good agreement between the classical and the modified approaches, with a significant reduction in computational cost when using the latter. However, depending on the number of assumed modes used in the simulation, the time consumption is very close to the flight duration and any additional processing required may compromise the real-time simulation. A reduced number of modes is, in this case, demanded to keep the real-time aptitude of the model. Therefore, additional strategies must be applied to the model, so full real-time capabilities are reached when using a larger number of assumed modes. These issues should then be taken into account and possible solutions need to be evaluated before embedding such a model into a full flight simulator. This may include the reduction in the number of aerodynamic strips, the use of a reduced number of assumed modes for the cases of interest, and the optimization of the routines and sub-routines. The use of more potent hardware may also be evaluated.

Another point of great relevance in this discussion is that the simplification in the computation of the generalized loads does not eliminate the matrix inversion of the apparent mass matrix and a more efficient form to calculate this matrix inversions is required. These inversions are one of the major vectors in the remaining online computations. Solutions to optimize this calculation may also lead to a significant reduction in the computational costs since the computational costs involved in this inversion increase dramatically with the order of the matrix, which in this case depends on the number of elastic modes retained. Consequently, the real-time simulation capabilities may be compromised. To conclude, although fast, the model is still of large order, because no sort of model order reduction technique is applied here.

## 5 REFERENCES

[1] Shearer, C. M. and Cesnik, C. E. (2008). Trajectory control for very flexible aircraft. *Journal of Guidance, Control, and Dynamics*, 31(2), 340–357.

[2] Qi, P. and Zhao, X. (2020). Flight control for very flexible aircraft using model-free adaptive control. *Journal of Guidance, Control, and Dynamics*, 43(3), 608–619.

[3] Silvestre, F. J., Guimarães Neto, A. B., Bertolin, R. M., et al. (2017). Aircraft control based on flexible aircraft dynamics. *Journal of Aircraft*, 54(1), 262–271.

[4] Damveld, H. J., Beerens, G. C., Van Paassen, M. M., et al. (2010). Design of forcing functions for the identification of human control behavior. *Journal of Guidance, Control, and Dynamics*, 33(4), 1064–1081.

[5] Muscarello, V., Quaranta, G., Masarati, P., et al. (2016). Prediction and simulator verification of roll/lateral adverse aeroservoelastic rotorcraft–pilot couplings. *Journal of Guidance, Control, and Dynamics*, 39(1), 42–60.

[6] Idan, M. and Merhav, S. (1990). Effects of biodynamic coupling on the human operator model. *Journal of Guidance, Control, and Dynamics*, 13(4), 630–637.

[7] Drewiacki, D., Silvestre, F. J., and Guimaraes Neto, A. B. (2018). Evaluation of aeroelastic effects on pilot-induced oscillations via pilot-in-the-loop simulations. In *2018 AIAA Atmospheric Flight Mechanics Conference*. p. 1016.

[8] Cook, R. G., Palacios, R., and Goulart, P. (2013). Robust gust alleviation and stabilization of very flexible aircraft. *AIAA journal*, 51(2), 330–340.

[9] Schwithal, J., Buch, J.-P., Seehof, C., et al. (2023). Simulating flexible aircraft in a full motion simulator. In *AIAA Aviation 2023 Forum*. p. 3318.

[10] Cesnik, C. and Su, W. (2005). Nonlinear aeroelastic modeling and analysis of fully flexible aircraft. In *46th AIAA/ASME/ASCE/AHS/ASC Structures, Structural Dynamics and Materials Conference*. p. 2169.

[11] Murua, J., Palacios, R., and Graham, J. M. (2010). Modeling of nonlinear flexible aircraft dynamics including free-wake effects. In *AIAA Atmospheric Flight Mechanics Conference*. p. 8226.

[12] Silvestre, F. J. and Luckner, R. (2015). Experimental validation of a flight simulation model for slightly flexible aircraft. *AIAA Journal*, 53(12), 3620–3636.

[13] Da Ronch, A., Badcock, K., Wang, Y., et al. (2012). Nonlinear model reduction for flexible aircraft control design. In *AIAA Atmospheric Flight Mechanics Conference*. p. 4404.

[14] Paulino, J., Da Ronch, A., Guimarães Neto, A., et al. On real-time simulation of flexible aircraft with physics-derived models.

[15] Paulino, J. (2020). *Studies on Model Order Reduction for Fast Simulation of Flexible Aircraft*. Ph.D. thesis, Intituto Tecnologico de Aeronautica.

[16] Klimmek, T. and Schulze, M. (2022). Development of a short medium range aircraft configuration for aeroelastic investigations using cpacs-mona. In *Deutscher Luft- und Raumfahrtkongress*.

[17] Wagner, H. (1925). Über die entstehung des dynamischen auftriebes von tragflügeln. *ZAMM-Journal of Applied Mathematics and Mechanics/Zeitschrift für Angewandte Mathematik und Mechanik*, 5(1), 17–35.

[18] Jones, R. T. (1938). Operational treatment of the nonuniform-lift theory in airplane dynamics.

[19] Jr, E. Y. (1966). Modified-strip-analysis method for predicting wing flutter at subsonic to hypersonic speeds. *Journal of Aircraft*, 3(1), 25–29.

## COPYRIGHT STATEMENT